R.J. Marks II, "Gerchberg's extrapolation algorithm in two dimensions",
Applied Optics, vol. 20, pp.1815-1820 (1981).

Gerchberg's extrapolation algorithm in two dimensions

Robert J. Marks II

Gerchberg's 1-D iterative extrapolation algorithm for bandlimited signals is generalized to two dimensions in two distinct ways. One generalization requires knowledge of the entire spectral pupil of the bandlimited image. The second requires only knowledge of two 1-D intervals formed by the vertical and horizontal projections of the pupil. For real bandlimited images of the low-pass type, this corresponds to knowing only the maximum x and y spatial frequencies of the image. The utilization of information of the known portion of the image in the extrapolation process is discussed for both algorithms. The second algorithm, reformulated discretely, is placed in closed form.

I. Introduction

Gerchberg[1] has presented a 1-D extrapolation algorithm for bandlimited signals which, in iterative form, requires only the operations of Fourier transformation and truncation.[2,3] This paper presents two distinctly different generalizations of Gerchberg's algorithm to two dimensions. The first generalization requires knowledge of the shape of the spectral pupil of the image to be extrapolated. The second requires only knowledge of the horizontal and vertical projections of the pupil. This latter algorithm, when discretely implemented, can be placed in closed form. In certain instances, the rectangular matrix formed by the sampled image is simply multiplied on both sides by an appropriately parameterized Sabri and Steenaart extrapolation matrix.[4] Implementations are presented in Ref. 5.

Much has recently been written on the instability (or ill-posedness or incompletely posedness) of extrapolation and super resolution algorithms.[3,6,7] Three observations are in order: (1) Analysis of algorithm stability, to date, deals with the error energy of the entire extrapolated signal. Extrapolation results should be better near to where the signal is known.[8] No allowance has yet been made for this conjecture. (2) There have been successful extrapolations of elementary signals and images utilizing unstable algorithms.[2,4,5] Required SNRs, however, are incredibly high. (3) There do exist completely posed extrapolation algorithms even according to present stability measures.[3]

II. Gerchberg's Algorithm

Let $u(x)$ have a spectrum

$$U(f_x) = F_x u(x) = \int_{-\infty}^{\infty} u(x) \exp(-j2\pi f_x x) dx$$

that is nonzero only over some region $\Omega_x \in f_x$. Defining the gate function

$$G_{\Omega_x}(f_x) = \begin{cases} 1; & f_x \in \Omega_x, \\ 0; & f_x \notin \Omega_x, \end{cases} \tag{1}$$

we say that u is bandlimited if

$$\int_{-\infty}^{\infty} G_{\Omega_x} df_x < \infty.$$

Let T_x denote an interval on x and define the spatial gate by

$$G_x(x) = \begin{cases} 1; & x \in T_x, \\ 0; & x \notin T_x. \end{cases}$$

The extrapolation problem is: given uG_x and Ω_x, determine u. The uniqueness of the result in the absence of noise is assured by well-known analyticity arguments.

Gerchberg's algorithm, in iterative form, can be summarized as follows: (1) Fourier transform uG_x; (2) truncate the spectrum by multiplying by G_{Ω_x}; (3) inverse transform; (4) discard that portion where the signal is known by multiplying by $(1 - G_x)$; (5) add in the known signal uG_x; and (6) Fourier transform, go to step 2, and repeat. From step 5, the Nth estimate can be written as $u_N = uG_x + H_x u_{N-1}$, where $u_0 = uG_x$, $H_x = (1 - G_x)B_x$, and the bandlimiting operator is defined by $B_x = F_x^{-1} G_{\Omega_x} F_x$. The convergence of u_N to u as N tends to infinity has been proven in three distinct ways.[1-3]

The author is with University of Washington, Department of Electrical Engineering, Seattle, Washington 98195.

Received 22 December 1980.
0003-6935/81/101815-06$00.50/0.

III. Generalization to Two Dimensions

Let $u(x,y)$ have a spectrum

$$U(f_x,f_y) = Fu(x,y) = \int_{-\infty}^{\infty}\int_{-\infty}^{\infty} u(x,y)\exp[-j2\pi(f_x x + f_y y)]dxdy.$$

Let Ω denote that region where U is nonzero. With reference to Fig. 1(d), let Ω_x and Ω_y denote the respective horizontal and vertical projections of Ω. The image u is said to be bandlimited if

$$\int_{-\infty}^{\infty}\int_{-\infty}^{\infty} G_{\Omega_x}G_{\Omega_y}df_x df_y < \infty,$$

where G_{Ω_y} is defined analogously to G_{Ω_x} in Eq. (1).

Let u be known within a region T. Define the corresponding aperture by

$$G_T = \begin{cases} 1; & (x,y) \in T, \\ 0; & (x,y) \in T. \end{cases}$$

Similarly, we define the spectral pupil as

$$G_\Omega = \begin{cases} 1; & (f_x,f_y) \in \Omega, \\ 0; & (f_x,f_y) \notin \Omega. \end{cases}$$

Then, in iterative form, Gerchberg's extrapolation algorithm can be straightforwardly generalized to two dimensions as follows: (1) Fourier transform uG_T; (2) multiply by spectral pupil G_Ω; (3) inverse transform; (4) discard the region where the image is known by multiplying by $(1 - G_T)$; (5) add in the known signal uG_T; and (6) Fourier transform, go to step 2, and repeat.

From the above description, the Nth estimate of u can be written from step 5 as $u_N = uG_T + (1 - G_T)B_\Omega u_{N-1}$, where $u_0 = uG_T$ and the bandlimiting operator is defined as $B_\Omega = F^{-1}G_\Omega F$. Equivalently, we can show inductively that

$$u_N = \sum_{n=0}^{N} H^n uG_T, \tag{2}$$

where $u_0 = uG_T$, and

$$H = (1 - G_T)B_\Omega. \tag{3}$$

Inspired by Papoulis's 1-D proof, proof of the convergence of u_N to u in Eq. (2) is offered in Appendix A for some nonseparable G_T's. Implementation of this algorithm on a coherent processor has recently been proposed.[9]

Note that Gerchberg's algorithm in this form is sensitive to the spectral pupil Ω. If this area is overestimated, erroneous spectral data are introduced in each iteration. Underestimation results in deletion of spectral information. In the next section, we present an alternate extension of Gerchberg's algorithm to two dimensions which requires knowledge of only Ω_x and Ω_y.

IV. Alternate Generalization

Consider the case where T consists of one or more disjoint islands as pictured in Fig. 1(a). Consider the 1-D function corresponding to the horizontal slice of uG_T at $y = y_0$. The duration of this function is dictated by T. To extrapolate the slice, however, we must also know its corresponding 1-D bandwidth interval. To determine this bandwidth interval, consider the spectrum in Fig. 1(d) and its inverse transform in y in Fig. 1(b). View the inverse transform from Fig. 1(d) to Fig. 1(b) as being performed along vertical slices. If the slice intersect Ω, we are inverse transforming a function with compact support. From the uncertainty principle of Fourier analysis, the result is a function which is bandlimited (in the 1-D sense) and is thus nowhere identically zero. If the slice does not intersect Ω, the inverse transform is, of course, zero. We thus conclude that the function in Fig. 1(b) is nonzero only within the shaded strip defined by the interval Ω_x. The bandwidth interval of the horizontal slice in Fig. 1(a) is, therefore, Ω_x, regardless of our choice of y_0. Generalizing, we conclude that two 1-D functions corresponding to two parallel slices of a bandlimited image have identical bandwidth intervals. Note, as shown in Fig. 1(c) for the vertical case, this interval can be disjoint.

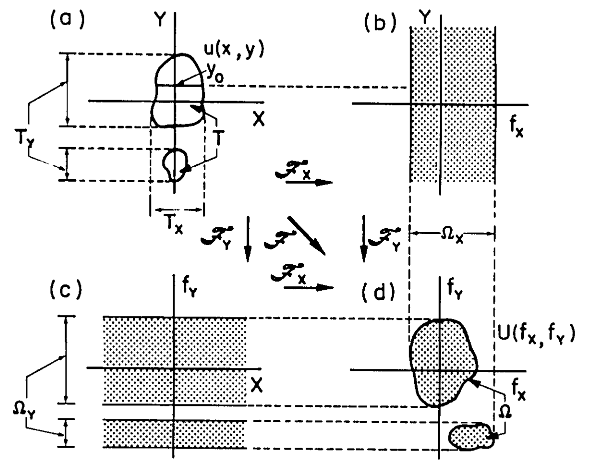

Fig. 1. Illustration of the equivalence of bandwidth intervals of parallel slices of a bandlimited image.

With knowledge of the duration and bandwidth intervals of each horizontal slice, we can apply Gerchberg's algorithm in one dimension to each horizontal slice in Fig. 1(a) and generate uG_y. Then, using the bandwidth interval Ω_y, this result can be vertically extrapolated to yield u over the entire (x,y) plane.

Note that, unlike the generalization in the previous section, this 2-D extrapolation scheme requires knowledge of only Ω_x and Ω_y (instead of Ω). For real bandlimited images of the low-pass type, Ω is a single centered symmetric area, and Ω_x and Ω_y can be determined from the maximum frequencies of the image in the x and y directions.

Mathematically, we can write the horizontal extrapolation within T_y as

$$uG_y = \sum_{m=0}^{\infty} H_x^m uG_T, \tag{4}$$

where

$$H_x = (1 - G_T)B_x,$$
$$B_\eta = F_\eta^{-1}G_{\Omega_\eta}F_\eta, \quad \eta = x,y. \tag{5}$$

Vertical extrapolation follows as

$$u = \sum_{n=0}^{\infty} H_y^n u G_y = \sum_{n=0}^{\infty} H_y^n \sum_{m=0}^{\infty} H_x^m u G_T, \tag{6}$$

where

$$H_y = (1 - G_y)B_y, \tag{7}$$

and G_y is the gate corresponding to T_y, the vertical projection of T [see Fig. 1(a)].

V. Algorithm Comparison

A contrast between the algorithms in Secs. III and IV is desirable. Algorithm 1, presented in Sec. III, requires knowledge of the entire spectral pupil region Ω. Algorithm 2 (Sec. IV) requires only knowledge of two projections of Ω: Ω_x and Ω_y. We are thus utilizing less information in this case and, as might be expected, will in some sense diminish algorithm effectiveness.

Consider Fig. 2 in which we wish to extrapolate uG_T. Using algorithm 2, the value of the extrapolation at point P_1, which lies within T_y, is determined solely from information gained from the intersection of uG_T with line L_1. Point P_2 lies in the area where we have extrapolated the horizontal extrapolation. Point P_3 is a hybrid case—formed both from information from uG_T and the horizontal extrapolation.

Thus we conclude that algorithm 2 extrapolates to a point using only 1-D slices of the original signal and/or previous extrapolations. Every point exterior to T, however, is related to every point within T. This observation is made clear upon inspection of point P_4 in Fig. 2. The extrapolated value at P_4 can, in principle, be determined from the intersection of any line through P_4 that intersects T.

Algorithm 1, on the other hand, clearly relates each interior point to each exterior point with the price that the entire spectral region, Ω, must be known.

VI. Algorithm 2 in Iterative Form

The algorithm in Sec. IV can be placed in iterative form by rewriting Eq. (6) as

$$u = \sum_{n=0}^{\infty} \sum_{m=0}^{n} H_y^{n-m} H_x^m u G_T,$$

and, in the spirit of iteration, define

$$u_N = \sum_{n=0}^{N} \sum_{m=0}^{n} H_y^{n-m} H_x^m u G_T. \tag{8}$$

Illustrations of the convergence of u_N to u are given in Appendix B. Note that

$$u_N = u_{N-1} + v_N, \tag{9}$$

where

$$v_N = \sum_{m=0}^{N} H_y^{N-m} H_x^m u G.$$

Furthermore,

$$v_N = H_y v_{N-1} + w_N, \tag{10}$$

where $w_N = H_x^N u G_T$. Obviously,

$$w_N = H_x w_{N-1}. \tag{11}$$

Equations (9)–(11) define an iterative form of Eq. (8) with initialization $u_0 = v_0 = w_0 = uG_T$.

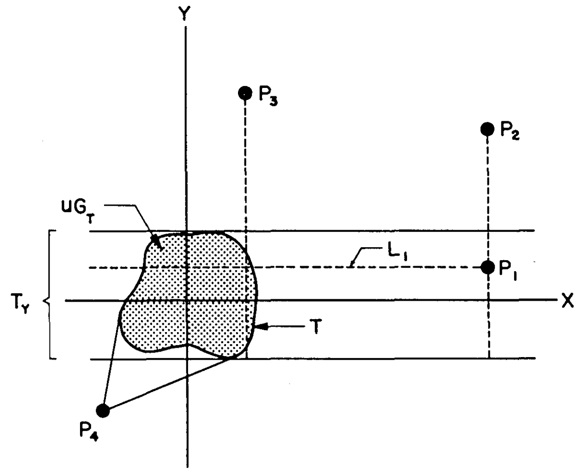

Fig. 2. Illustration of the contribution of the known portion of an image to its extrapolation.

VII. Algorithm 2 in Closed Form

In this section, the image extrapolation algorithm in Sec. IV is placed in closed form. Consider first the case where $G_T = G_x G_y$ is a rectangle centered about the origin. Let uG_T be sampled and placed in a rectangular matrix $\hat{u}_T$. Then the result of the Mth 1-D horizontal extrapolated image, $\hat{u}_M$, is, from Eq. (4),

$$\hat{u}_M = \sum_{m=0}^{M} \hat{u}_T (\mathrm{H}_x')^m, \tag{12}$$

where the prime denotes matrix transposition. The H_x matrix is the discrete equivalent of Eq. (5) within T_y: $\mathrm{H_x} = (\mathrm{I} - \hat{G}_x)\mathrm{B}_x$, where I denotes the identity matrix, and $\hat{G}_\eta$, $\eta = x,y$, is a square gate matrix corresponding to G_η. It contains ones and zeros appropriately placed on the diagonal and is elsewhere zero. The B_x matrix, corresponding to B_x, is

$$\mathrm{B}_x = (\mathrm{D}^{-1}\hat{G}_{\Omega_x}\mathrm{D})',$$

where D is the discrete Fourier transform matrix, and $\hat{G}_{\Omega_x}$ is the square gate matrix corresponding to G_{Ω_x}.

From (6), we can vertically extrapolate to give

$$\hat{u}_{NM} = \sum_{n=0}^{N} \mathrm{H}_y^n \hat{u}_T, \tag{13}$$

where

$$\mathrm{H}_y = (I - \hat{G}_y)\mathrm{D}^{-1}\hat{G}_{\Omega_y}\mathrm{D}.$$

Note that, if $T_x = T_y$ and $\Omega_x = \Omega_y$, then $\mathrm{H}_x = \mathrm{H}_y'$. Substituting Eq. (12) into Eq. (13) gives

$$\hat{u}_{NM} = \mathrm{E}_N \hat{u}_T \mathrm{E}_M', \tag{14}$$

where

$$\mathrm{E}_L = \sum_{r=0}^{L} \mathrm{H}_\eta^r; \quad (l,r,\eta) = (M,n,x), (N,m,y).$$

E_L is recognized as one of Sabri and Steenaart's 1-D extrapolation matrices.[4] It can be found digitally through straightforward matrix multiplication.

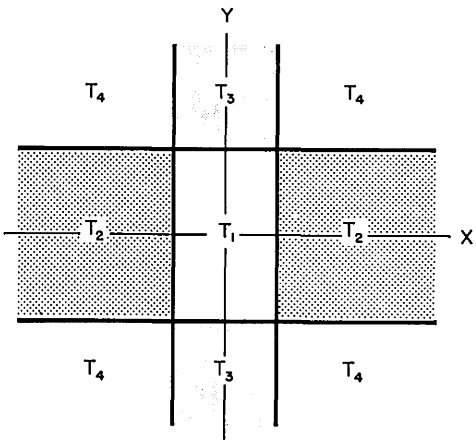

Fig. 3. Regions of convergence.

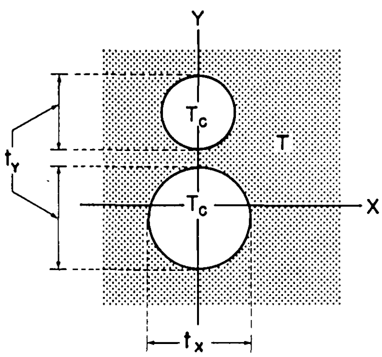

Fig. 4. Parametrization illustration for the case where an image is known outside of a finite region.

The second form of the extrapolation matrix can be found form matrix inversion. Assuming convergence, we have

$$E_\eta \equiv \lim_{L\to\infty} E_L = (I - H_\eta)^{-1}.$$

Then Eq. (14) becomes

$$\hat{u} = E_y \hat{u}_T E_x'. \tag{15}$$

Some example implementations of this closed form 2-D extrapolation scheme are given in Ref. 5.

Note that the extrapolation matrices in both Eqs. (14) and (15) are parametrized by T_η and Ω_η; $\eta = x,y$. Since each horizontal slice of uG_T is known over the same interval T_x and has the same bandwidth, Ω_x, the same extrapolation matrix is used for each slice. The same is true for the vertical extrapolation. Note again that, if $T_x = T_y$ and $\Omega_x = \Omega_y$, then $E_y = E_x'$.

A straightforward generalization holds when G_T has a finite T_x and T_y but is not separable. For a given y within T_y, we can extrapolate each horizontal slice of uG_T using an extrapolation matrix parametrized by the same bandwidth interval, Ω_x, and the interval corresponding to the intersection of the horizontal line at our chosen y with G_T. Once uG_T is extrapolated into a horizontal strip within T_y, vertical extrapolation can be performed with a single extrapolation matrix parametrized by T_y and Ω_y.

The algorithm, in fact, is applicable to all T such that a single vertical or horizontal extrapolation does not fill the entire plane. Consider, for example, Fig. 3 and let $T = T_4$. The horizontal extrapolation would fill T_3. The vertical extrapolation would then fill T_1 and T_2. Proof of convergence of Eq. (8) for the case where $T = T_2$ is contained in Appendix B.

VIII. Augmentation of Algorithm 2

Algorithm 2 is not applicable to the case where T is chosen such that a single vertical or horizontal extrapolation fills the plane. Such a case is when $T = T_1 U T_4$ in Fig. 3. An alternate approach is thus necessary.

Consider first the case where u is known outside a finite region as illustrated in Fig. 4. Denote the region where u is not known by T_c. Let t_x and t_y be the corresponding horizontal and vertical projections.

One method of extrapolation for this case is simply to extrapolate vertically within the t_x interval. Specifically, for $x \in t_x$,

$$u = uG_T + (1 - G_T) \sum_{n=1}^{\infty} H_y^n u G_T,$$

where, instead of Eq. (7), we define

$$H_y = (1 - G_T) B_y. \tag{16}$$

Note that the image outside of the vertical strip defined by t_x is not even used in this scheme.

A second method of extrapolation, equivalent to averaging, uses both the t_x and t_y strips:

$$u = uG_T + \tfrac{1}{2}(1 - G_T) \sum_{n=1}^{\infty} (H_x^n + H_y^n) u G_T,$$

with operator definitions in Eqs. (5) and (16). This relation can be straightforwardly placed in iterative form:

$$u_N = u_{N-1} + \tfrac{1}{2} v_N + \tfrac{1}{2} w_N,$$
$$v_N = G_{t_y} H_x v_{N-1},$$
$$w_N = G_{t_x} H_y w_{N-1},$$

with initializations

$$u_0 = G_{t_x} G_{t_y} u G_T,$$
$$v_0 = G_{t_y} u G_T,$$
$$w_0 = G_{t_x} u G_T,$$

where

$$G_{t_\eta}(\eta) = \begin{cases} 1; & \eta \in t_\eta; \quad \eta = (x,y), \\ 0; & \eta \in t_\eta. \end{cases}$$

One might conclude that better extrapolation can be gained by averaging the contributions of a larger and larger number of radial strips. Radial extrapolation could be similarly applied to the algorithm in Sec. VI. Each radial strip, however, requires knowledge of another projection of Ω. Thus, in the limit, we would require complete knowledge of Ω.

This work was generously supported by the National Science Foundation under grant ENG-79-08009.

Appendix A

Our purpose here is to prove the convergence of u_N to u in Eq. (2) as N tends to infinity. In all cases, we will assume Ω to be a $2W_x \times 2W_y$ rectangle centered about the origin. Define

$$G_c = \begin{cases} 1; & |\eta| \le c/2, \\ 0; & |\eta| > c/2, \end{cases} \tag{A1}$$

where $(c,\eta) = (a,x)$ or (b,η). In this case, the familiar integral equation,[10,11]

$$\lambda_r \psi_r(\eta) = 2W_\eta \int_{-c/2}^{c/2} \psi_r(\xi) \operatorname{sinc} 2W_\eta (\eta - \xi) d, \tag{A2}$$

[where $(r,c,\eta) = (p,a,x)$ or (q,b,y) and $\operatorname{sinc} x = \sin\pi x/\pi x$], has as a solution the set of prolate spheroidal wave functions parametrized by the space–bandwidth product $2W_\eta C$. The eigenvalues have the property that

$$0 < \lambda_r < 1. \tag{A3}$$

The eigenfunctions ψ_r in Eq. (A2) are obviously bandlimited and are thus not altered by filtering:

$$\psi_r(\eta) = 2W_\eta \int_{-\infty}^{\infty} \psi_r(\xi) \operatorname{sinc} 2W_\eta(\eta - \xi) d\xi. \tag{A4}$$

Equations (A2) and (A4) can be equivalently stated in operator form as

$$B_\eta \psi_r G_c = \lambda_r \psi_r, \tag{A5}$$

$$B_\eta \psi_r = \psi_r. \tag{A6}$$

Any bandlimited image with the specified bandwidth region, Ω, can be written as

$$u = \sum_{pq} u_{pq} \psi_p \psi_q. \tag{A7}$$

The determination of u_{pq} from uG_T will be specified in each example to follow.

Case 1: Consider first the nonseparable case when u is known outside of an $a \times b$ rectangle. That is, $G_T = 1 - G_a G_b$. The expansion coefficients can then be found from

$$u_{pq} = \frac{1}{1 - \lambda_p \lambda_q} \int_{-\infty}^{\infty} \int u G_T \psi_p \psi_q dx dy. \tag{A8}$$

Using Eqs. (A5), (A6), and (2), we can inductively show that, for $n \ge 1$,

$$H^n \psi_p \psi_q G_T = (1 - G_T)(\lambda_p \lambda_q)^{n-1}(1 - \lambda_p \lambda_q)\psi_p \psi_q.$$

Substituting Eq. (A7) into Eq. (2) thus yields

$$\begin{aligned} u_N &= uG_T + (1 - G_T) \sum_{pq} u_{pq} \psi_p \psi_q (1 - \lambda_p \lambda_q) \sum_{n=1}^{N} (\lambda_p \lambda_q)^{n-1} \\ &= uG_T + (1 - G_T) \sum_{pq} u_{pq} \psi_p \psi_q [1 - (\lambda_p \lambda_q)^N]. \end{aligned} \tag{A9}$$

From Eq. (A3) the term $(\lambda_p \lambda_q)^N \to 0$ as $N \to \infty$, and Eq. (A9) becomes Eq. (A7).

Case 2: Here we choose $G_T = 1 - G_a(1 - G_b)$. Thus, u is known everywhere but within two semi-infinite vertical strips $T = T_1 U T_3 U T_4$ in Fig. 3. The proof here is the same as above, except, instead of Eq. (A8), the expansion coefficients are determined from

$$u_{pq} = \frac{1}{1 - \lambda_p(1 - \lambda q)} \int_{-\infty}^{\infty} \int u G_T \psi_p \psi_q dx dy.$$

Equation (A9) remains identical, except that, instead of $[1 - (\lambda_p \lambda_q)^N]$, we obtain the term $1 - [\lambda_p(1 - \lambda_q)]^N$, which, due to Eq. (A3), also converges to unity.

Similar proof can be generated for the cases where $G_T = G_a G_b$, $1 - (1 - G_a)(1 - G_b)$, $G_a(1 - G_b)$, etc.

Appendix B

Case 1: In this section the alternate form of Gerchberg's iterative extrapolation algorithm in two dimensions [Eq. (8)] is proved first for the case where $G_T = G_a G_b$. Thus, $G_x = G_a$ and $G_y = G_b$. Also, let Ω have single symmetric projections of $2W_x$ and $2W_y$. We begin by rewriting Eq. (8) as

$$u_N = uG_T + \sum_{n=1}^{N} H_x^n u G_T + \sum_{n=1}^{N} H_y^n u G_T + \sum_{n=1}^{N} \sum_{m=1}^{n-1} H_y^{n-m} H_x^m u G_T. \tag{B1}$$

As we shall demonstrate, each of these four terms corresponds to the disjoint regions on the x-y plane illustrated in Fig. 3. The first term, uG_T, is our original image and thus exists only in region $T = T_1$. The second term corresponds to the horizontal extrapolation result and exists only in region T_2. The third term similarly exists only in T_3. The final term corresponds to the extrapolated extrapolation and exists only in region T_4.

We will now examine the terms individually. Using the results of Appendix A, we can express u as in Eq. (A7), where

$$u_{pq} = \frac{1}{\lambda_p \lambda_q} \int_{-\infty}^{\infty} u G_T \psi_p \psi_q dx dy.$$

Consider first the second term in Eq. (B1). From Eqs. (5), (A5), and (A6), we can inductively show that, for $n \ge 1$,

$$H_x^n u G_T = G_b(1 - G_a) \sum_{pq} u_{pq} (1 - \lambda_p)^{n-1} \lambda_p \psi_p \psi_q. \tag{B2}$$

The second term thus becomes

$$\sum_{n=1}^{N} H_x^n u G_T = G_b(1 - G_a) \sum_{pq} u_{pq} \psi_p \psi_q [1 - (1 - \lambda_p)^N]. \tag{B3}$$

Using Eq. (A3), this expression converges to u via Eq. (A7) over region T_2 as N tends to ∞. A similar analysis can be applied to show the convergence of the third term to u in region T_3.

To analyze the fourth term in Eq. (B1), we first use Eq. (B2) with n replaced by m to obtain $H_x^m uG$. Then applying H_y^{n-m} we can inductively show that, for $n > m > 0$,

$$H_y^{n-m}H_x^m uG = (1 - G_a)(1 - G_b)\sum_{pq} u_{pq}\psi_p\psi_q s_{pq}(n,m),$$

where

$$s_{pq}(n,m) = \lambda_p\lambda_q(1-\lambda_p)^{m-1}(1-\lambda_q)^{n-m-1}.$$

If we can show that

$$S_N = \sum_{n=1}^{N}\sum_{m=1}^{n} s_{pq}(n,m) \tag{B4}$$

tends to unity as $N \to \infty$, convergence to u in T_4 is assured.

If $\lambda_p \neq \lambda_q$, we can apply the geometric series formula to Eq. (B4) twice and obtain

$$S_N = \frac{1}{\lambda_p - \lambda_q}\{\lambda_p(1-\lambda_q)[1-(1-\lambda_q)^N] - \lambda_q(1-\lambda_p)[1-(1-\lambda_p)^N]\}.$$

Using Eq. (A3), we conclude that

$$\lim_{N\to\infty} S_N = 1.$$

The occurence of the relation $\lambda_p = \lambda_q$ will appear when $a = b$. Then

$$S_N = (N+1)(1-\lambda_p)^N - N(1-\lambda_p)^{N-1} + 1.$$

Due to Eq. (A3), this relation also approaches unity.

Case 2: A similar proof can be generated for $G_T = G_a(1 - G_b)$. Consider again Eq. (B1). For our given G_T, the first term exists only in region $T = T_3$ in Fig. 3. The second term will converge in region T_4, the third in T_1, and the last in T_2. The proof is identical to Case 1, except that $1 - G_b$ replaces G_b and $1 - \lambda_q$ replaces λ_q.

Similar proofs can also be generated when a single vertical or horizontal extrapolation does not fill the entire plane. These include $G_T = (1 - G_a)(1 - G_b)$ and $(G_a - G_b)^2$.

References

1. R. W. Gerchberg, Opt. Acta **21**, 709 (1974).
2. A. Papoulis, IEEE Trans. Circuits Syst. **CAS-22**, 735 (1975).
3. D. C. Youla, IEEE Trans. Circuits Syst. **CAS-25**, 694 (1978).
4. M. S. Sabri and W. Steenaart, IEEE Trans. Circuits Syst. **CAS-25**, 74 (1978).
5. D. K. Smith, "Extrapolation of 2-D Bandlimited Images," M.S. Thesis, U. Wash. Dept. Electrical Engineering (1980).
6. G. A. Viano, J. Math Phys. **17**, 1160 (1976).
7. R. G. Wiley, IEEE Trans. Commun. **COM-27**, 251 (1979).
8. W. K. Pratt, *Digital Image Processing* (Wiley, New York, 1968), pp. 437–440.
9. R. J. Marks II, Appl. Opt. **19**, 1670 (1980).
10. D. Slepian and H. O. Pollak, Bell Syst. Tech. J. **40**, 43 (1961).
11. G. T. DiFrancia, J. Opt. Soc. Am. **59**, 799 (1969).

Books *continued from page 1814*

(sodium and mercury), fluorescent lamps, and flashbulbs. Measurement of light concentrates on intensities in terms of luminous intensity of a source and at a surface. There is also a short section on diagrams of light distributions caused by housings for light sources. The effect of materials on light begins with the index of refraction, polarization, reflection, interference, and absorption. Color and color mixing cover the concepts of complementary colors, colors as perceived by the eye, and color mixing by additive and subtractive methods.

Chapter 6, the Optical Appearance of Materials, makes use of the concepts developed in the first five chapters. It begins with a more rigorous discussion of the index of refraction. Anisotropic indices are touched on lightly and their relation to the appearance and preparation of pigments is discussed. Since pigments are usually in powdered form, one uses an average of the indices if the original material is anisotropic. The index of refraction is directly associated with the "hiding power" which depends on the light scattered from the pigment-vehicle (oil) surfaces. If the difference in index between the vehicle and pigment is large, the hiding power is large because the pigment will scatter light. If the indices are identical there is no scattering and the hiding power is small. However, the hiding power is also affected by the amount of pigment: if the pigment density is low, the hiding power may be low even though the difference in indices is large. Furthermore, the hiding power may change with age because of an increase in the index of the vehicle or a decrease in index of the pigment.

Anomalous dispersion is discussed briefly because some pigments have their anomalous dispersion regions in the visible, for example, solid cyanin.

Particle size of the pigments also affects the opacity and surface appearance of paintings because of the scattering. There is a short discussion of Rayleigh scattering, followed by a section on pigment particles and how their average size can affect color saturation.

Chapter 6 continues on the subjects of reflectance, transmittance, and absorption of light. Glossy and matte surfaces can affect perceived color, as can transparent coatings and films. Glass, glazes, and enamels are discussed, followed by fibers and woven materials.

Chapters 7–9 discuss the origin of color in organic materials and photoreactions. Chapter 7 is a short course in atomic and molecular structure and chemical bonding and leads to the subject of electronic transitions in organic molecules which is the source of color in organic materials. Chapter 8 takes up the subject of organic dyes, how they are applied, their historical classification, and their chemical structure. Chapter 9 discusses the decomposition of organic materials by light, the chemical principles involved, rates of photochemical reactions, and mechanisms of photochemical reactions of dyes. In addition, photochemical reactions in paper, textiles, wood, varnish, and oils are discussed. How to minimize photochemical effects and the future of natural organic materials conclude the chapter.

Chapters 10 and 11 discuss the origin of color in inorganic compounds, pigments, and colored glass. Chapter 10 is to inorganic compounds what Chap. 7 is to organic compounds. In it are discussions of covalent bonds, charge transfer transitions, electronic configuration of ions, the *d–d* transition, and the effect of crystal structure on color. It closes with a short section on the effect of particle size and concentrations on color.

Chapter 11 is concerned with artist's pigments and colored glass. Mixing of pigments and their decomposition by light is discussed. Colors in glass and glaze and the effect on them of light concludes this chapter.

Chapter 12 discusses the photographic process. Photo-image materials are restricted to the silver halides. The action of light on silver halide grains, the spectral sensitivity of this reaction, and sensitizers required to enable photographing reds and oranges, and developing and fixing images are presented. Photographic materials can also degrade with time because organic materials are usually

continued on page 1839